HHS Public Access

Author manuscript

J Immunol. Author manuscript; available in PMC 2023 April 15.

Published in final edited form as:

J Immunol. 2022 April 15; 208(8): 2008–2018. doi:10.4049/jimmunol.2000945.

IL-27 enhances γδ T cell-mediated innate resistance to primary hookworm infection in the lungs

Arjun Sharma[§,†,$], **Jason B. Noon**[§,$], **Konstantinos Kontodimas**[§], **Lucien P. Garo**[§], **Johannes Platten**[†], **Lee J. Quinton**[§,@], **Joseph F. Urban Jr**[*], **Christoph Reinhardt**[†], **Markus Bosmann**[§,†,‡]

[§]Pulmonary Center, Department of Medicine, Boston University School of Medicine, Boston, Massachusetts, 02118, USA

[†]Center for Thrombosis and Hemostasis, University Medical Center of the Johannes Gutenberg University Mainz, 55131, Mainz, Germany

[‡]Research Center for Immunotherapy (FZI), University Medical Center of the Johannes Gutenberg-University Mainz, 55131, Mainz, Germany

[*]United States Department of Agriculture, Agricultural Research Service, Beltsville Agricultural Research Center, Animal Parasitic Diseases Laboratory and Beltsville Human Nutrition Research Center, Diet, Genomics, and Immunology Laboratory, Beltsville, Maryland, 20705, USA

[@]Division of Infectious Disease and Immunology, Department of Medicine, University of Massachusetts Chan Medical School, Worcester, MA, 01605, USA

Abstract

Interleukin-27 (IL-27) is a heterodimeric IL-12 family cytokine, formed by non-covalent association of the promiscuous EBI3 subunit and selective p28 subunit. IL-27 is produced by mononuclear phagocytes and unfolds pleiotropic immune-modulatory functions through ligation to IL-27 receptor alpha (IL-27RA). While IL-27 is known to contribute to immunity and to limit inflammation following various infections, its relevance for host defense against multicellular parasites is still poorly defined. Here, we investigated the role of IL-27 during infection with the soil-transmitted hookworm, *Nippostrongylus brasiliensis*, in its early host intrapulmonary life cycle. IL-27(p28) was detectable in broncho-alveolar lavage fluids of C57BL/6J wild type (WT) mice on day 1 after subcutaneous inoculation. IL-27RA expression was most abundant on lung-invading γδ T cells. Il27ra$^{-/-}$ mice showed increased lung parasite burden together with aggravated pulmonary hemorrhage and higher alveolar total protein leakage as a surrogate for epithelial/vascular barrier disruption. Conversely, injections of recombinant mouse (rm)IL-27

Corresponding Author: Markus Bosmann, Associate Professor of Medicine. Pathology & Laboratory Medicine, Pulmonary Center, Department of Medicine, Boston University School of Medicine, Boston, Massachusetts, 02118, USA. Phone: +1-617-358-1225. FAX: +1-617-638-5227. mbosmann@bu.edu.

Author Contributions

A.S., J.B.N., K.K. and J.P. designed and performed experiments and analyzed data. L.P.G., J.U., and C.R. contributed to experimental designs and provided helpful comments. M.B. conceived and supervised the study, designed experiments, interpreted data and provided funding. A.S., J.B.N. and M.B. wrote the manuscript, which was further edited by L.P.G., J.U., L.J.Q. and C.R.

[$]These authors contributed equally to the work.

Disclosures

The authors have no financial conflicts of interest.

into WT mice reduced lung injury and parasite burden. In multiplex screens, higher airway accumulations of IL-6, TNFα, and MCP-3 (CCL7) were observed in Il27ra$^{-/-}$ mice, while rmIL-27 treatment showed a reciprocal effect. Importantly, γδ T cell numbers in airways were enhanced by endogenous or administered IL-27. Further analysis revealed a direct anti-helminthic function of IL-27 on γδ T cells, as adoptive intratracheal transfer of rmIL-27-treated γδ T cells during primary *N. brasiliensis* lung infection conferred protection in mice. In summary, this report demonstrates protective functions of IL-27 to control the early lung larval stage of hookworm infection.

Keywords

Inflammation; parasitic-helminth; cytokines; immunology; Acute respiratory distress syndrome (ARDS)

Introduction

Hookworms are soil-transmitted intestinal nematodes that have a critical stage in parasitic development within the host lungs (1). After molting from an infectious third stage larvae (L3) to a L4 stage within the lungs, hookworms ascend the trachea and are swallowed, ultimately infecting the small intestine where they transiently remain as egg-laying adults. In the small intestine, hookworms rupture vessels and feed on blood, which is the cause of clinical hookworm disease characterized by iron-deficiency anemia in humans and livestock. Over 500 million people worldwide are infected with hookworms (2, 3) and among all parasites, hookworms are behind only malaria for the leading causes of iron-deficiency anemia globally (4–7). Although there are anti-helminthic drugs available for treating hookworms (8, 9), people are rapidly reinfected in endemic areas due to insufficient immunity and high vulnerability for secondary infections (10). Importantly, there is not a single licensed hookworm vaccine (11), stressing the value of understanding protective immunity to hookworm infections.

The murine hookworm, *Nippostrongylus brasiliensis*, is a model for human hookworm disease, particularly for the stage of infection within the lungs, which occurs on days 1 and 2 after subcutaneous inoculation into mice (12). On day 3, larvae transition to the small intestine and remain as adult worms until a period of expulsion beginning around day 7. There are many publications that indicate the importance of the canonical type 2 response involving cytokines such as IL-4, IL-5, IL-13 and RELMβ, along with group 2 innate lymphoid cells (ILC2s), type 2 T helper (Th2) cells, alternatively activated macrophages, eosinophils, basophils, mast cells and goblet cells in resistance to *N. brasiliensis* during secondary lung infection (13). However, knowledge on primary infection in the lungs is sparse (14–19). Resistance to primary hookworm infections in rodents has focused largely on the small intestine and, in the *N. brasiliensis* model, is well-characterized by canonical type 2-driven expulsion mediated by ILC2s and Th2 cells (13), as well as type 2 γδ T (γδ T2) cells (i.e., intestinal intraepithelial T lymphocytes; IELs) (20). Although much less is known about primary resistance in the lungs to hookworm infections, in the *N. brasiliensis*

infection model, IL-17A, neutrophils, alternatively activated macrophages, and γδ T cells are involved (14, 16, 21).

IL-27 is a heterodimeric cytokine composed of a unique p28 α-subunit and a promiscuous EBI3 β-subunit (22). EBI3 is shared with IL-35 (23, 24). The IL-27 receptor is also a heterodimer composed of a unique IL-27 receptor α-subunit (IL-27RA, WSX-1) and a gp130 β-subunit that is shared with several other cytokine receptors (22, 25, 26). IL-27 is well-described to exert acute pro-inflammatory effects, enhancing type 1 responses, particularly $CD8^+$ cytotoxic lymphocytes (CTLs) and natural killer (NK) cells, thus enhancing protective immunity to intracellular pathogens and various cancers (27, 28). Consistent with IL-27 enhancing type 1 responses, IL-27 directly suppresses the expansion and activation of ILC2s during the lung repair phase of primary *N. brasiliensis* infections (29). A more rapid intestinal expulsion is seen in the absence of IL-27 activities in both the *N. brasiliensis* infection model (studying $Ebi3^{-/-}$ mice) and in response to the mouse whipworm, *Trichuris muris* (studying $Il27ra^{-/-}$ mice) (29, 30). Importantly, there are no publications on IL-27 during early primary *N. brasiliensis* infections in the lungs, or any other helminth infection.

Given that type 2-associated immune responses are involved in limiting later stages of primary *N. brasiliensis* infection in the lungs (13), and IL-27 is well known to antagonize such responses (26, 31), we initially hypothesized that IL-27 may limit resistance to primary *N. brasiliensis* infections in the lungs by suppressing type 2 responses. Interestingly, however, we found that IL-27 enhanced resistance to early stages of primary *N. brasiliensis* infections in the lungs in association with increased expansion of γδ T cells, which were also found to express much higher levels of IL-27RA compared both $CD4^+$ Th cells and $CD8^+$ CTLs. Further analysis revealed a direct anti-helminthic function of IL-27 on γδ T cells, as adoptive intratracheal transfer of rmIL-27-treated γδ T cells during primary *N. brasiliensis* lung infection conferred protection in mice. Thus, we have demonstrated that there are mechanisms of innate resistance to pulmonary hookworm infection beyond type 2 responses.

Materials and Methods

Mice

All procedures with mice were approved by the Institutional Animal Care and Use Committee of the Boston University and performed in compliance with the guidelines of the National Institutes of Health. $Il27ra^{-/-}$ mice (B6N.129P2-$Il27ra^{tm1Mak}$/J; on C57BL/6NJ background), C57BL/6NJ mice, and C57BL/6J mice were obtained from the Jackson Laboratory (Bar Harbor, ME). The mice were bred and genotyped at the animal facilities of Boston University under specific pathogen-free conditions and a controlled light/dark cycle. Male and female mice at 8–12 weeks of age were used for experiments.

N. brasiliensis cultures and inoculations

N. brasiliensis infective third stage larvae (L3) were separated from copro-cultures and prepared for inoculations according to an established protocol (12). Mice were injected

subcutaneously in the flank with n=500 L3 in 0.1 mL of sterile PBS (Thermo Fisher Scientific, Waltham, MA).

Recombinant IL-27 treatment during N. brasiliensis infection

For treatment with recombinant mouse (rm) IL-27, mice were administered either rmIL-27 (100 ng/mouse) or mock control (0.1% BSA in PBS) i.p. The first dose was given on day 0 along with *N. brasiliensis* inoculation, while the second dose was given on day 1 post-inoculation (p.i.)

Adoptive transfer of γδ T cells during N. brasiliensis infection

For γδ T cell adoptive transfer experiments, γδ T cells were isolated from the spleens of naïve C57BL/6J mice using the magnetic bead TCRγ/δ$^+$ T Cell Isolation Kit (Miltenyi Biotec, Germany) according to the manufacturer's instructions. Purity was confirmed to be ~95% by flow cytometry. Single cell suspensions of γδ T cells in PBS were stimulated with rm-IL-27 (100 ng/mL) or mock (PBS) treated for 30 min at 37°C, and 100,000 γδ T cells per mouse were injected intratracheally (i.t.) 12 hours after inoculation with N. *brasiliensis*. For i.t. injections, mice were anesthetized with a xylazine-ketamine solution and given subcutaneously 1 ml NaCl 0.9% post-operatively for fluid resuscitation.

Alveolar and lung tissue parasite burdens

To measure alveolar parasite burden, inoculated mice were euthanized by CO_2 overdose, and three broncho-alveolar lavages (BAL) were collected before vital organ removal. For the first BAL, 1 mL PBS containing 1X HALT Protease Inhibitor Cocktail/EDTA (Thermo Fisher Scientific, Waltham, MA) was collected into a 1.5 mL tube. PBS only was used for the second and third BAL and were collected into a 50 mL tube. The first BAL was centrifuged at 400 × g for 8 min at room temperature and the cell-free supernatant was collected as BAL fluid (BALF) and stored at −80°C for later analysis. The pellet of BAL cells containing *N. brasiliensis* larvae was then resuspended in PBS and transferred to the 50 mL tube along with the additional BAL collections. The combined BAL was then diluted to 30 mL with PBS and transferred to a 100 mm petri dish with grids drawn on the bottom surface. All intact live *N. brasiliensis* larvae, indicated by larval mobility, were counted under 20X magnification (AmScope, Irvine, CA). *N. brasiliensis* debris were excluded, while obviously dead (i.e., immobile) and deteriorating larvae were counted as dead parasites. The suspension of BAL cells and *N. brasiliensis* larvae was then transferred back to the 50 mL tube and centrifuged at 800 × g for 8 min at 4°C. The supernatant was removed down to 10 mL. Next, the BAL cell pellet was resuspended, transferred to a 15 mL tube and centrifuged as before. The supernatant was removed down to 0.5 mL, and the BAL cell pellet was transferred to a 1.5 mL tube before further analysis.

To measure parasite burden in lung tissues, lungs were collected from inoculated mice after BAL collections into 35 mm petri dishes. Lungs were minced with surgical scissors, resuspended in a 5 mL slurry of 1% agarose at 37°C, and then pipetted onto a flattened layer of cheesecloth. Once solidified, the cheesecloth was rolled up and placed in a submerging vessel of 45 mL PBS in a 50 mL tube, with a small piece of the cheesecloth secured between

the tube and lid, and then incubated in 37°C overnight. Larvae that migrated out of the lung tissue/agarose were counted under 20X magnification.

Gut parasite burdens

To enumerate total gut parasite burden, the small and large intestines were excised, total contents were flushed with PBS, and tissues were cut longitudinally to expose the lumen. Parasite counts along the lumen were then counted under a tissue dissecting microscope (AmScope, Irvine, CA) as described by Mchedlidze et al. (29). The recovered PBS was also examined for dislodged worms.

Alveolar injury

BALF total protein was measured with a Pierce BCA Protein Assay Kit (Thermo Scientific). Alveolar hemorrhage was assessed as described elsewhere (32), but with the following modifications. A 6X 2-fold serial dilution (8000–250 μg/mL) of human hemoglobin (Sigma, St. Louis, MO) was prepared, and 50 μL of each standard and BALF sample were added to duplicate wells of a 96-well plate. A volume of 100 μL of 6% sodium dodecyl sulfate (Sigma, St. Louis, MO) was added to all wells and resuspended several times. The absorbance at 560 nm was measured with a Tecan Infinite M Nano plate reader (Tecan, Männedorf, Switzerland), and alveolar hemorrhage (i.e., total amount of hemoglobin recovered in BALF) was determined from the standard curve generated by Magellan V 7.2 (Tecan, Männedorf, Switzerland) software.

ELISA & multiplex bead-based immunoassay

IL-27(p28) in BALF was measured with a mouse IL-27 p28/IL-30 DuoSet ELISA kit (R&D Systems, Minneapolis, MN), according to the manufacturer's instructions. The absorbance at 450 nm was measured with a Tecan Infinite M Nano plate reader, and concentration was determined from the standard curve generated by Magellan software.

A multiplex bead-based immunoassay (Cytokine & Chemokine 26-Plex Mouse ProcartaPlex™ Panel 1, Thermo Fisher Scientific) was used for simultaneous quantification of the following cytokines/chemokines: IL-1β, IL-2, IL-4, IL-5, IL-6, IL-9, IL-10, IL-12p70, IL-13, IL-17A, IL-18, IL-22, IL-23, IL-27, GROα (CXCL-1), IP-10 (CXCL-10), MCP-1 (CCL-2), MCP-3 (CCL-7), MIP-1α (CCL-3), MIP-1β (CCL-4), MIP-2 (CXCL-2), RANTES (CCL-5), Eotaxin (CCL-11), GM-CSF, IFNγ, and TNF-α (33). All samples from bead-based assays were performed using a LiquiChip-200 instrument (Qiagen, Hilden, Germany) using Bio-Plex Manager v6.1 software for quantification.

Flow Cytometry

Fresh BAL cells (3 × 1 mL) were collected from inoculated mice as described above. In multiple experiments using our standard operating procedures, >99% of BAL cells were found to be negative for fixable viability dye eFluor 780 (eBioscience, ThermoFisher Scientific), and hence, all BAL cells were considered alive. BAL cells collected in a 15 mL tube were centrifuged at 800 × g at 4°C for 8 min. Cells were transferred to 1.5 mL tubes and incubated in the dark for 30 min, using the following mouse antibody staining cocktails: Myeloid-lymphocyte common lineage panel – TruStain FcX (anti-CD16/32)

(clone: 93; dilution: 1:100, BioLegend, San Diego, CA), CD45-Pacific Blue (clone: 30-F11; dilution 1:200, BioLegend), Ly6G-APC (clone: 1A8; dilution: 1:400, BioLegend), Siglec-F-APC/Cy7 (clone: E50-2440; dilution: 1:200, BioLegend), CD11c-Alexa Fluor 488 (clone: N418; dilution: 1:600, BioLegend), CD3-BUV737 (clone: 145-2C11; dilution: 1:100, BD Biosciences, San Jose, CA), CD19-PE/Cy7 (clone: 6D5; dilution: 1:100, BioLegend), NK1.1-PerCP/Cy5.5 (clone: PK136; dilution: 1:100, BioLegend), IL-27RA-PE (clone: 2918; dilution: 1:100, BD Biosciences), rat IgG2a, κ isotype PE control (clone: R35–95; dilution: 1:100, BD Biosciences); T cell panel – TruStain FcX (anti-CD16/32) (clone: 93; dilution: 1:100, BioLegend), CD3-BUV737 (clone: 145-2C11; dilution: 1:100, BD Biosciences), TCRβ chain-PE/Cy7 (clone: H57-597; dilution: 1:100, BioLegend), CD4-Alexa Fluor 488 (clone: RM4-5; dilution 1:400, BioLegend), CD8a-APC/Cy7 (clone: 53–6.7; dilution: 1:100, BioLegend), TCRγδ-APC (clone: GL3; dilution: 1:00, BioLegend), NK1.1-PerCP/Cy5.5 (clone: PK136; dilution: 1:100, BioLegend), IL-27RA-PE (clone: 2918; dilution: 1:100, BD Biosciences) or PE Rat IgG2a, κ Isotype Control (clone: R35–95; dilution: 1:100, BD Biosciences). All antibodies were diluted in FACS buffer prepared from sterile PBS and supplemented with 0.25% (w/v) BSA, 0.02% (w/v) sodium azide, and 2 mM EDTA. The stained cells were rinsed in FACS buffer, and then fixed in 2% paraformaldehyde (Santa Cruz Biotechnology, Dallas, TX) at room temperature for 20 min in the dark. Stained/fixed cells were centrifuged as described before, resuspended in FACS buffer and transferred to a FACS tube containing 20 μL of CountBright Absolute Counting Beads (ThermoFisher Scientific). For all single-stained compensation controls, we used OneComp eBeads Compensation Beads (Invitrogen, Waltham, MA) according to the manufacturer's instructions. Flow cytometric acquisition of samples was performed on a BD LSR II flow cytometer with BD FACSDiva software. Preparation and analyses of final plots were performed in FlowJo v10.

Reagents

Recombinant mouse IL-27 (<1.0 EU per 1 μg of the rmIL-27 protein by the LAL method) was purchased from R&D systems.

Data analysis

Statistical analyses were performed, and graphs were prepared in Prism v7–9 (GraphPad Software). Data in bar graphs are depicted as mean ± standard error of the mean (S.E.M.), with overlaid symbols representing values from individual mice. The numbers of mice per group are indicated as circles in the figures and are representative or pooled from 2 independent experiments. Two-group single comparisons were made with a t-test. Multiple comparisons were made with one-way or two-way ANOVA followed by Tukey's post hoc test. P values <0.05 were considered significant. P values <0.1 were considered as a trend.

Results

IL-27(p28) is transiently elevated in the alveolar space during primary N. brasiliensis infection of the lungs

While *N. brasiliensis* infection is well known to induce an eosinophilic- and Th2 cell-dependent immune response, the role of the immune-modulatory cytokine, IL-27, is not well

described in the pulmonary state of the hookworm infection cycle. To test if IL-27(p28) was released during primary *N. brasiliensis* infection of the lungs, C57BL/6J mice (wild type, WT) were inoculated with n=500 *N. brasiliensis* L3, and EDTA-plasma was collected on days 0, 1, 2, 6, and 9 following inoculation. BALF was collected on days 0, 1, 2, and 9 post-inoculation (p.i.). Circulating IL-27(p28) was not detectable in EDTA-plasma by ELISA at any of the studied time points, even though all mice were confirmed to be highly infected with an average of 40,000 eggs per gram of feces on day 6 p.i. (data not shown). However, in BALF, IL-27(p28) was elevated by ~3-fold on day 1 p.i. compared to day 0 ($P<0.0001$, Fig. 1A). The concentrations of IL-27(p28) returned to normal levels by day 2 (Fig. 1A). Thus, these results indicate that IL-27(p28) is transiently released specifically in the alveolar space during primary *N. brasiliensis* infection of the lungs. The bulk of IL-27 may avidly bind to its receptor for rapid clearance or altogether escape detection in cell-free BALF.

IL-27RA is highly expressed on T cells in the alveolar space during primary pulmonary N. brasiliensis infection

To study if IL-27RA is expressed on invading immune cells in the broncho-alveolar space during primary *N. brasiliensis* infection of the lungs, we first confirmed leukocyte dynamics in BAL from WT mice on days 0, 1, and 2 p.i. with *N. brasiliensis* larvae. Within the myeloid lineage (Fig. S1A), we recovered approximately ~10,000 $CD11c^{+}Siglec\text{-}F^{+}$ resident alveolar macrophages per mouse in BAL on day 0 in sham mice (Fig. S1B). In addition, while no $Ly6G^{+}$ neutrophils or $CD11c^{-}Siglec\text{-}F^{+}$ eosinophils were present in BAL of sham mice, the numbers of these myeloid cells substantially increased over the course of 2 days following inoculation with *N. brasiliensis* L3 (Fig. S1B). Furthermore, within the lymphocyte lineage (Fig. 1B), while few cells were detectable in day 0 p.i. BAL, accumulations of $CD19^{+}CD3^{-}$ B cells, $CD19^{-}CD3^{+}$ T cells and $CD19^{-}CD3^{-}NK1.1^{+}$ NK cells were detected on day 1 and further elevated on day 2 (Fig. 1C). Thus, myeloid and lymphoid cells tended to increase in the alveolar space during the natural course of primary *N. brasiliensis* infection.

Essentially none of the three myeloid cell types (neutrophils, eosinophils, alveolar macrophages) present in BAL after inoculation were found to express IL-27RA at any time point evaluated (Fig. S1C). However, on day 2 p.i. an average of 80.2%, 56.1% and 23.1% of T cells, NK cells and B cells were $IL\text{-}27RA^{+}$, respectively. These percentages were similar on both day 1 and 2 p.i. (Fig. 1D, E). Geometric mean fluorescence intensities (gMFIs) of IL-27RA were 1.5-fold greater on T cells on day 2 compared to day 1 p.i., suggesting T cell-specific upregulation of IL-27RA (Fig. 1F, G), while IL-27RA gMFI was similar on NK cells and B cells at the two time points studied (Fig. 1F). Moreover, IL-27RA gMFI was ~3-fold higher on T cells compared to NK cells and B cells. Hence, the frequency and magnitude of IL-27RA expression was greatest on $CD19^{-}CD3^{+}$ T cells in the alveolar space during primary *N. brasiliensis* infection of the lungs.

We next evaluated the numbers of different T cell subsets in the alveolar space during primary pulmonary *N. brasiliensis* infection, and for their expression of IL-27RA. Both $TCR\beta^{+}CD4^{+}$ Th cells and $TCR\beta^{+}CD8^{+}$ CTLs became considerably more abundant than

TCRβ^{-}TCRγδ^{+} γδ T cells p.i., while none of these lymphocyte populations were present in BAL from uninfected mice (Fig. 2A, B). The numbers of Th cells, CTLs and γδ T cells further increased from day 1 to day 2 p.i. (Fig. 2B). Moreover, the majority of all three cell types was IL-27RA^{+} (Fig. 2C, D). There was a significantly higher percentage of IL-27RA^{+} γδ T cells compared to IL-27RA^{+} CTLs and IL-27RA^{+} Th cells, while there was not a significant difference between IL-27RA^{+} CTLs and IL-27RA^{+} Th cells (Fig. 2D). Furthermore, γδ T cells showed significantly higher IL-27RA gMFI compared to both CTLs and Th cells, and CTLs presented with significantly higher IL-27RA gMFI compared to Th cells (Fig. 2E). Thus, IL-27RA was most prevalent and most highly expressed on γδ T cells, but Th cells and CTLs dominated the T cell population in the alveolar space during primary *N. brasiliensis* infection of the lungs.

IL-27 signaling enhances resistance to primary N. brasiliensis infection in the lungs

To further elucidate the role of IL-27, the course of the *N. brasiliensis* infection in mice deficient in IL-27RA was analyzed. Consistent with previous characterizations (34), we found no global defects in immune development in naïve Il27ra$^{-/-}$ mice (Fig. S2). Flow cytometric analyses of lymphocytes (Fig. S2A) revealed similar numbers of B Cells, γδ T cells, CD4^{+} T cells, CD8^{+} T cells, and NK cells between C57BL/6NJ WT and Il27ra$^{-/-}$ mice (Fig. S2B). As expected, Il27ra$^{-/-}$ mice lacked expression of IL-27RA in these populations, in contrast to WT mice (Fig. S2C). Interestingly, γδ T cells expressed particularly high levels of IL-27RA in the spleens of naïve WT mice (Fig. S2C, D), complementing our findings in lungs of *N. brasiliensis*-infected mice (Fig. 2D, E). Immunophenotyping of splenic neutrophils, monocytes, macrophages, and eosinophils (Fig. S2E) also revealed unaltered frequencies in naïve Il27ra$^{-/-}$ mice (Fig. S2F), along with lack of IL-27RA expression on both Il27ra$^{-/-}$ and WT cells (Fig. S2G). Furthermore, gating on all CD19^{-}CD3^{-}NK1.1^{-}CD49b^{-} non-lymphoid cells revealed a lack of IL-27RA expression on other cell types in WT mice (Fig. S2H, S2I). Together, these findings support Il27ra$^{-/-}$ mice as a viable tool to study how IL27 signaling may mediate specific immune responses.

To determine if IL-27 had a beneficial or detrimental role during primary *N. brasiliensis* infection of the lungs, we first inoculated Il27ra$^{-/-}$ mice and WT mice with 500 *N. brasiliensis* L3 and compared alveolar parasite burden, hemorrhage, and total protein on day 2 p.i.. Strikingly, Il27ra$^{-/-}$ mice showed a significant ~2-fold increase in live parasite counts in BAL compared to WT mice (Fig. 3A). Furthermore, we confirmed this increase in live parasite counts corresponded to a decrease in dead parasite burden (Fig. 3A), indicating a defect in pathogen clearance in alveolar spaces when IL-27RA was absent. Consistent with parasites collected in BAL, we found a ~2-fold increase in live parasites and decrease in dead parasites within the lung tissue of Il27ra$^{-/-}$ mice (Fig. 3A, 3B). To evaluate the severity of parasite-induced lung injury, we determined hemoglobin concentrations in BAL as a marker for airway hemorrhage and broncho-alveolar total protein as a surrogate endpoint for the disturbance of epithelial/vascular barrier function. A significant ~2-fold increase in alveolar hemorrhage in Il27ra$^{-/-}$ mice compared to WT mice was observed, in line with the greater parasite burden of Il27ra$^{-/-}$ mice (Fig. 3C). Moreover, also consistent with the greater parasite burden, a moderate but significant increase in total protein leakage was

detected in the BALF of Il27ra$^{-/-}$ mice (Fig. 3D), indicating an increase in proteinaceous edema.

Next, we tested whether administration of exogenous IL-27 would further reduce the severity of *N. brasiliensis* infection in the lungs of WT mice. For this, we administered 100 ng recombinant mouse IL-27 (rmIL-27) intraperitoneally on days 0 and 1 p.i. in WT mice and compared alveolar parasite burden and injury with a carrier/mock-treated group. The rmIL-27 treatment significantly reduced live larvae counts in BAL and lung to less than half of mock controls (Fig. 3E, 3F). Accordingly, the decrease in live parasite counts in the BAL and lungs of treated mice corresponded to an increase in dead parasite counts (Fig. 3E, F). In addition, alveolar hemorrhage was significantly decreased to almost half of mock controls (Fig. 3G), while a very slight decrease in total alveolar protein leakage was statistically insignificant (Fig. 3H). We also validated an earlier report that IL-27 enhanced parasite burden during subsequent intestinal stages of disease (29), as we observed the opposite trend —decreased live parasite burden in Il27ra$^{-/-}$ mice (Fig. S5A) and increased live parasite burden (Fig. S5B) in rmIL-27-reated mice—in the gut at day 4 p.i. Taken together, these results indicate that both endogenous IL-27/IL-27RA signaling and therapeutic recombinant IL-27 enhanced innate resistance to primary *N. brasiliensis* infection during the early lung larval stage.

IL-27 modulates the local presence of proinflammatory cytokines and chemokines.

To characterize the influence of IL-27 on the local milieu of inflammatory mediators, we employed a high-sensitivity, bead-based multiplex assay to quantify the concentrations of 26 cytokines and chemokines (Fig. 4, S3). Il27ra$^{-/-}$ mice along with WT control mice were infected with *N. brasiliensis* L3 and BALF was collected 2 days later. Significant differences were observed for 5 of 26 mediators. IL-6 concentrations were ~2-fold greater in Il27ra$^{-/-}$ mice (Fig. 4A). TNFα was also significantly increased in Il27ra$^{-/-}$ mice, although levels were near the lower detection limit of the assay, possibly owing to the time point chosen (Fig. 4A). The macrophage- and T cell-driving chemokine, MCP-3, was 2-fold higher in Il27ra$^{-/-}$ mice (Fig. 4A). In addition, we detected a trend towards lower concentrations for IL-23 ($p = 0.09$), a proinflammatory cytokine which is known to modulate T cell activity (Fig. 4A). Moreover, lower IL-10 concentrations and higher IL-17 amounts were detected (Fig. S3A) in Il27ra$^{-/-}$ mice, which is consistent with the known requirement of IL-27 signaling to induce IL-10 from T cells and to suppress IL-17 responses in other disease models (35–37). Other differential cytokine and chemokine levels may be an indirect result of increased parasite burden or general inflammation, rather than a direct consequence of loss of IL-27 signaling. For example, increased expression of IL-6 and TNF-α significantly correlated with greater numbers of live larvae in BAL found in Il27ra$^{-/-}$ mice (Fig S4A).

To further elaborate on the findings with Il27ra$^{-/-}$ mice, we measured inflammatory mediators in BALF of *N. brasiliensis*-infected WT mice two days after a treatment regimen of rmIL-27 (100 ng i.p. on days 0 and 1 p.i.) or mock injections. IL-6 was again observed to be present in abundant quantities, especially when considering the substantial dilution of alveolar lining fluid introduced by the lavage procedure (Fig. 4B). In contrast to the effect of IL-27 deficiency, IL-6 was suppressed by the addition of rmIL-27 (Fig. 4B). Likewise, mice

that received rmIL-27 were found to have lower TNFα and MCP-3 (Fig. 4B). Interestingly, no increase in IL-27 itself was detected in BALF 2 days after rmIL-27 injection (Fig. S3B), suggesting clearance prior to that time point. In fact, we noticed a trend for suppressed (endogenous) IL-27 after injection, possibly attributable to a post-excitation phenomenon. A pattern similar to Il27ra$^{-/-}$ mice was also observed following rmIL-27-treatment, whereby changes in cytokine and chemokine levels tended to correspond to parasite burdens (Fig S4B).

Absence of IL-27 signaling decreases the expansion of γδ T cells in the alveolar space during primary N. brasiliensis infection

As T cells by far have the highest expression of IL-27RA (Fig. 1E–G), and all three T cell subsets evaluated express IL-27RA (albeit highest on TCRβ^{-}TCRγδ^{+} γδ T cells; Fig. 2C–E), we next compared the percentage and number of all three T cell subsets in day 2 p.i. BAL between WT and Il27ra$^{-/-}$ mice. Compared to WT mice, we observed a significant 1.4-fold reduction in the percentage of TCRβ^{-}TCRγδ^{+} γδ T cells, a mild reduction in the percentage of TCRβ^{+}CD8^{+} CTLs, and a slight increase in the percentage of TCRβ^{+}CD4^{+} Th cells (Fig. 5A, B) in Il27ra$^{-/-}$ mice. Most importantly, BALs from Il27ra$^{-/-}$ mice exhibited a 1.5-fold reduction in the absolute number of γδ T cells, while the counts of Th cells and CTLs were unchanged (Fig. 5C). The absolute numbers of macrophages, neutrophils, eosinophils, T cells, B cells, and NK cells were unaffected in Il27ra$^{-/-}$ mice (Fig S5C). Thus, these findings support a prominent role for IL-27 in enhancing the expansion of γδ T cells in the alveolar space during primary *N. brasiliensis* infection.

Following these observations, we next tested if IL-27 directly promotes anti-helminthic γδ T cell responses to protect against *N. brasiliensis* infection of the lung. First, we treated mice with rmIL-27 during *N. brasiliensis* infection, and found that IL-27 enhanced both the frequency (Fig. 6A) and absolute number (Fig. 6B) of γδ T cells in BALs on day 2 p.i. As in Il27ra$^{-/-}$ mice, absolute numbers of other broad lymphocyte and myeloid cells remained unchanged (Fig. S5D), suggesting IL-27 preferentially affected γδ T cells in this disease context. Because γδ T cell numbers in the lung appeared undisturbed in uninfected Il27ra$^{-/-}$ mice (Fig. S5E), we next asked if IL-27 might enhance γδ T cell numbers by upregulating the expression of chemokine receptors on γδ T cells that would promote recruitment to the lungs in infected mice. Interestingly, we did not find any significant change in the expression of several important chemokine receptors known to be expressed by γδ T cells (38–40), including CXCR1, CXCR3, CCR2, and CCR5 (Fig. S5F–G). To determine if there was a direct impact of IL-27 on γδ T cells, we next employed an adoptive intratracheal transfer approach (Fig. 6C). γδ T cells were isolated from naïve WT donors, treated *in vitro* with or without rmIL-27, and transferred to recipient WT mice, that had been inoculated with *N. brasiliensis* larvae 12 hours earlier (Fig. 6C). Mice which received rmIL-27-treated γδ T cells showed a significant decrease in live parasite burden and increase in dead parasite counts in the BALF and lung (Fig. 6D, E). Together, these data demonstrate that the impact of IL-27 on γδ T cells is capable of conferring protection to lung infection of *N. brasiliensis*, indicating γδ T cells are key mediators of this protective IL-27 effect.

Discussion

In this report, we have identified a functional role for IL-27 signaling in protective immune defense against hookworm larvae, which migrate from the pulmonary vasculature into the airways.

IL-27RA was expressed on all airway-invading lymphocytes, albeit differentially based on cellular subset. IL-27RA was particularly abundant on γδ T cells compared to other innate and adaptive lymphocytes, suggesting this cell type as a prominent target for IL-27-mediated defense in the current setting. To this end, genetic deficiency of IL-27RA resulted in greater parasite burden and more severe lung injury, whereas the opposite was true following rmIL-27 treatment. These findings were associated with differences in local proinflammatory cytokines and γδ T cell numbers in Il27ra$^{-/-}$ mice. Adoptive intratracheal transfer of rmIL-27-treated γδ T cells during primary *N. brasiliensis* lung infection conferred protection in mice, revealing a direct anti-helminthic function of IL-27 on γδ T cells.

Innate immunity to helminths is widely accepted to be limited to expulsion, a canonical type 2 response orchestrated by Th2 cells, ILC2s, and γδ T2 IECs that, in the case of hookworm infections, is not initiated until the adult stage of the life cycle in the small intestine (13, 20, 41, 42). Innate immune mechanisms responsible for defense against helminth infections within the lungs have received much less attention, likely due to the gut being the conserved final destination for the majority of geohelminths. Even among studies on intrapulmonary helminths, the focus has remained on immune responses after initial lung infection and concurrent with subsequent infection of the gut, especially regarding anti-helminthic ILC2 accumulation in the lung which arises about a week post-initial infection (15, 29, 43–48). We demonstrated that there are mechanisms of innate resistance to hookworm infection in the lungs that are not necessarily associated with type 2 responses. As a key activator of pulmonary resistance to hookworms, we found that IL-27 was transiently induced for expansion of γδ T cells in the alveolar space that contributed to killing parasitic larvae directly and/or indirectly prior to their transition to the small intestine.

Indeed, examining both BAL and lung tissue, we found an increase in the number of dead parasites in mice treated with systemic rmIL-27 (Figs. 3E, F) or adoptive intratracheal transfer of rmIL-27-stimulated γδ T cells (Figs. 6D, E), along with a corresponding decrease in IL-27ra$^{-/-}$ mice (Fig. 3 A, B), suggesting IL-27 activates effective killing of lung-resident parasites. Although IL-27 has been shown to promote wound healing (49), it seems unlikely that a decrease in local tissue inflammation and larvae dissemination is responsible for the protective effect of IL-27 on parasite burden in the lung. We did not employ secondary challenges with percutaneous and intradermal inoculation of L3 to elicit host skin responses (50, 51). The subcutaneous route of injection of *N. brasiliensis* would have allowed the parasitic L3 to begin transit along arterioles within hours toward the lung (12) bypassing much of cutaneous immunity. Rather, it seems a direct effect of IL-27-activated γδ T cells, or an indirect influence of γδ T cells on local cells such as alveolar macrophages, may be responsible for parasite killing (16). Together, our results strongly suggest that the role of

IL-27 in the lung stage of hookworm infection is the opposite of the stage in the gut, being anti-parasitic for the former and pro-parasitic for the latter (29, 52).

Consistent with a strong role for local innate γδ T cells in the lungs, IL-27-dependent changes occurred within the first two days of infection. This suggests that IL-27's beneficial effects stem from alterations in innate immunity, especially given the time required for antigen-specific T cell responses. Yet, cytokine-induced T cells can modulate inflammation independently of their T cell receptor (53, 54), such that their accumulation and higher absolute numbers relative to γδ T cells in the airspaces may still contribute to the inflammatory milieu in some capacity.

Regarding alveolar cytokine and chemokine changes, the downregulation of IL-6 production by IL-27 (Fig. 4) may be a direct effect, since lymphocytes can both produce and respond to IL-6 (55, 56). Alternatively, changes in IL-6 may occur as an indirect consequence of IL-27RA-expressing NK cells and T cells dispatching signals to control IL-6 synthesis in other non-lymphocytic cells. The precise role of IL-6 in lung injury and pulmonary inflammation appears to be somewhat dependent on the disease model (57, 58).

The chemokine, MCP-3 (CCL7), shares 71% sequence similarity with MCP-1 (CCL2) and binds to the CCR2 receptor (59, 60). CCR2 is constitutively expressed not only on monocytes/macrophages, but also on T cells, including IL-17 producing γδ T cells (61). However, the higher concentrations of MCP-3 in Il27ra$^{-/-}$ mice during hookworm infection seem to contradict the lower influx of γδ T cells in these mice (Fig. 4A vs. Fig. 5C). The increased MCP-3 may rather represent an ineffective compensatory feedback loop to bring T cell numbers back up when too low. IL-27 itself is not a chemokine, but gp130-induced JAK/STAT1/STAT3 signaling may regulate expression of chemokines, chemokine receptors and T cell migration (62, 63). Another possibility is that elevated MCP-3 is secondary to the increase in pathogen burden resulting from IL-27 deficiency, making the precise roles of MCP-3 speculative at present.

The lack of clear upregulation of several key chemokine receptors, including CCL2 (64–66), on the surface of γδ T cells further underscores the need for more work elucidating these trafficking mechanisms. IL-27 might modulate γδ T cell recruitment by regulating other chemokine receptors or cell adhesion molecules. Alternatively, IL-27 may increase γδ T cell numbers in the lung through other means, such as by modulating γδ T cell activation, proliferation, or survival. The few studies characterizing any direct effects of IL-27 on γδ T cells suggest these are possibilities (67, 68). Almost all the work on IL-27 in T cells has focused on conventional CD4$^+$ and CD8$^+$ T cells (26, 69–71) and more investigation is needed to untangle basic IL-27 downstream signaling mechanisms in γδ T cells.

IL-27 is almost exclusively produced by macrophages and dendritic cells (26, 72). For example, we have previously shown that during endotoxemia, depletion of mononuclear phagocytes decreases circulating IL-27 levels *in vivo* by >80% (72). Here, we have detected IL-27RA expression on all lung lymphocyte subpopulations during hookworm infection, which is consistent with abundant evidence highlighting the responsiveness and functional roles of IL-27 in T cells and B cells (26, 73). On the other hand, we did not observe

IL-27RA expression on mouse myeloid cells in lung and spleen, while receptor expression and IL-27 responsiveness has been reported for human neutrophils and human monocytes (74, 75). We caution that none of the earlier reports have assessed IL-27RA expression in a cell-specific capacity (as accomplished by flow cytometry in the present study), but instead relied on RT-PCR or western blotting of cell lysates, making conclusive determination of cellular source somewhat speculative.

The mechanisms of helminth-induced IL-27 expression remain unclear. No dedicated class of pattern recognition receptors for helminth recognition has been identified so far. Helminth-derived chitin, proteoglycans, lipids, and excretory-secretory products may be recognized by TLRs and C-type lectins (40, 76–79). In addition, danger associated molecular patterns (DAMPs), when released during helminth-induced tissue injury, could act as endogenous ligands for TLRs (and other receptors), thereby inducing MYD88/TRIF-dependent IL-27 production (72, 80–82). Furthermore, γδ T cells can be activated by DAMPs from mitochondria (83).

The regulatory role of IL-27 for the host immune defense against helminths does not appear to be limited to hookworms. Dual deficiency of IL-27RA and IL-10 rescues the great susceptibility of IL-10 single knockout mice for intestinal pathology and infection caused by the whipworm, *Trichuris muris* (84). *Strongyloides stercolaris*, the causative threadworm of strongyloidiasis, infects more than 50 million people worldwide and infection results in a moderate but significant increase of IL-27 in human plasma, which decreases after anti-helminthic treatment (85). In human whole blood cultures of infected individuals re-stimulated with recombinant *S. stercolaris* NIE antigen, the neutralization of IL-27 using antibodies increases the frequencies of all $CD4^+$ T helper cell subsets (T_{h1}-T_{h22}), $CD8^+$ T cells and modulates cytokine levels (86). *Ascaris lumbricoides* antigen has been shown to induce IL-27 release from PBMCs in adults/the elderly as compared to neonates/children from an endemic cohort in Sub-Saharan Africa with a 30% prevalence of hookworm and other parasite infections (87). Altogether, these observations suggest an important influence of IL-27 on host outcome in a variety of settings of helminthic infections.

While we describe in this report that recombinant IL-27 reinforced the anti-helminthic host defense in the lungs, the feasibility of proposing its administration as an effective therapy is highly speculative. First, the efficacy observed in our studies was only around 50% for reduction of the lung larvae burden in IL-27-treated mice, although this could be improved by further dose optimization. Secondly, the skin penetration of hookworm larvae in humans usually is unnoticed, such that any window of therapeutic efficacy may be too difficult to rely on. Thirdly, another report showed that a non-viral minicircle DNA vector injected intra-venously for recombinant expression of IL-27 resulted in higher numbers of adult *N. brasiliensis* in the intestinal tract (29). This finding and our presented data (Fig. 3, S5A–B) imply that the role of IL-27 is either protective or detrimental depending on the stage of the hookworm infection cycle and host tissue environment. It appears that more sophisticated manipulations would be needed to specifically enhance IL-27-dependent protective immunity in the lung. IL-27 may be an interesting factor to explore for developing adjuvants for vaccines that target the early lung stage of human hookworms (11). Vaccine adjuvants would need to be tailored to locally induce IL-27 (88–90), or to up-regulate

IL-27RA expression and IL-27 responsiveness of lung resident lymphocyte subpopulations (91).

In conclusion, the presented work expands on the emerging role of IL-27 as a critical factor of host defense and immune regulation against hookworm infections, and provides a strong rationale for future studies to elucidate the relatively uncharted area of fundamental IL-27-activated mechanisms within γδ T cells during the pulmonary stage of parasitic infection. In the future, more research will be needed to fully uncover the intricate molecular mechanisms of host-helminth interactions as a basis for developing innovative treatment and control strategies against this neglected tropical disease.

Supplementary Material

Refer to Web version on PubMed Central for supplementary material.

Acknowledgments

We thank Deepthi Sree Vamaraju for assisting with the Figure preparation and manuscript editing. We thank Kara Farquharson for reading and editing the final draft of the manuscript.

Funding

Research reported in this publication was supported by the National Heart, Lung, and Blood Institute of the National Institutes of Health under Award Number T32HL007035, the Federal Ministry of Education and Research (01EO1503 to M.B. and C.R.), the Deutsche Forschungsgemeinschaft (BO3482/3-3, BO3482/4-1 to M.B. and RE-3450/5-2 to C.R.), and a project grant from the Boehringer Ingelheim Foundation (Consortium Grant “Novel and neglected cardiovascular risk factors” to C.R.). C.R. was awarded a fellowship from the Gutenberg Research College. The content is solely the responsibility of the authors and does not necessarily represent the official views of the funding agencies.

References

1. Loukas A, Hotez PJ, Diemert D, Yazdanbakhsh M, McCarthy JS, Correa-Oliveira R, Croese J, and Bethony JM. 2016. Hookworm infection. Nat Rev Dis Primers 2: 16088. [PubMed: 27929101]
2. Pullan RL, Smith JL, Jasrasaria R, and Brooker SJ. 2014. Global numbers of infection and disease burden of soil transmitted helminth infections in 2010. Parasit Vectors 7: 37. [PubMed: 24447578]
3. Herricks JR, Hotez PJ, Wanga V, Coffeng LE, Haagsma JA, Basanez MG, Buckle G, Budke CM, Carabin H, Fevre EM, Furst T, Halasa YA, King CH, Murdoch ME, Ramaiah KD, Shepard DS, Stolk WA, Undurraga EA, Stanaway JD, Naghavi M, and Murray CJL. 2017. The global burden of disease study 2013: What does it mean for the NTDs? PLoS Negl Trop Dis 11: e0005424. [PubMed: 28771480]
4. Brooker S, Hotez PJ, and Bundy DA. 2008. Hookworm-related anaemia among pregnant women: a systematic review. PLoS Negl Trop Dis 2: e291. [PubMed: 18820740]
5. Smith JL, and Brooker S. 2010. Impact of hookworm infection and deworming on anaemia in non-pregnant populations: a systematic review. Trop Med Int Health 15: 776–795. [PubMed: 20500563]
6. Hotez PJ, Brooker S, Bethony JM, Bottazzi ME, Loukas A, and Xiao S. 2004. Hookworm infection. N Engl J Med 351: 799–807. [PubMed: 15317893]
7. Kassebaum NJ, and Collaborators GBDA. 2016. The Global Burden of Anemia. Hematol Oncol Clin North Am 30: 247–308. [PubMed: 27040955]
8. Hotez PJ, Bundy DAP, Beegle K, Brooker S, Drake L, de Silva N, Montresor A, Engels D, Jukes M, Chitsulo L, Chow J, Laxminarayan R, Michaud C, Bethony J, Correa-Oliveira R, Shuhua X, Fenwick A, and Savioli L. 2006. Helminth Infections: Soil-transmitted Helminth Infections and Schistosomiasis. In Disease Control Priorities in Developing Countries. nd, Jamison DT, Breman

JG, Measham AR, Alleyne G, Claeson M, Evans DB, Jha P, Mills A, and Musgrove P, eds, Washington (DC).

9. Anderson R, Truscott J, and Hollingsworth TD. 2014. The coverage and frequency of mass drug administration required to eliminate persistent transmission of soil-transmitted helminths. Philos Trans R Soc Lond B Biol Sci 369: 20130435. [PubMed: 24821921]
10. Bethony J, Brooker S, Albonico M, Geiger SM, Loukas A, Diemert D, and Hotez PJ. 2006. Soil-transmitted helminth infections: ascariasis, trichuriasis, and hookworm. Lancet 367: 1521–1532. [PubMed: 16679166]
11. Noon JB, and Aroian RV. 2017. Recombinant subunit vaccines for soil-transmitted helminths. Parasitology 144: 1845–1870. [PubMed: 28770689]
12. Camberis M, Le Gros G, and Urban J Jr. 2003. Animal model of Nippostrongylus brasiliensis and Heligmosomoides polygyrus. Curr Protoc Immunol Chapter 19: Unit 19 12.
13. Nair MG, and Herbert DR. 2016. Immune polarization by hookworms: taking cues from T helper type 2, type 2 innate lymphoid cells and alternatively activated macrophages. Immunology 148: 115–124. [PubMed: 26928141]
14. Sutherland TE, Logan N, Ruckerl D, Humbles AA, Allan SM, Papayannopoulos V, Stockinger B, Maizels RM, and Allen JE. 2014. Chitinase-like proteins promote IL-17-mediated neutrophilia in a tradeoff between nematode killing and host damage. Nat Immunol 15: 1116–1125. [PubMed: 25326751]
15. Cardoso V, Chesne J, Ribeiro H, Garcia-Cassani B, Carvalho T, Bouchery T, Shah K, Barbosa-Morais NL, Harris N, and Veiga-Fernandes H. 2017. Neuronal regulation of type 2 innate lymphoid cells via neuromedin U. Nature 549: 277–281. [PubMed: 28869974]
16. Chen F, Wu W, Millman A, Craft JF, Chen E, Patel N, Boucher JL, Urban JF Jr., Kim CC, and Gause WC. 2014. Neutrophils prime a long-lived effector macrophage phenotype that mediates accelerated helminth expulsion. Nat Immunol 15: 938–946. [PubMed: 25173346]
17. Harvie M, Camberis M, and Le Gros G. 2013. Development of CD4 T Cell Dependent Immunity Against N. brasiliensis Infection. Front Immunol 4: 74. [PubMed: 23518620]
18. Sotillo J, Sanchez-Flores A, Cantacessi C, Harcus Y, Pickering D, Bouchery T, Camberis M, Tang SC, Giacomin P, Mulvenna J, Mitreva M, Berriman M, LeGros G, Maizels RM, and Loukas A. 2014. Secreted proteomes of different developmental stages of the gastrointestinal nematode Nippostrongylus brasiliensis. Mol Cell Proteomics 13: 2736–2751. [PubMed: 24994561]
19. Min B, Prout M, Hu-Li J, Zhu J, Jankovic D, Morgan ES, Urban JF Jr., Dvorak AM, Finkelman FD, LeGros G, and Paul WE. 2004. Basophils produce IL-4 and accumulate in tissues after infection with a Th2-inducing parasite. J Exp Med 200: 507–517. [PubMed: 15314076]
20. Inagaki-Ohara K, Sakamoto Y, Dohi T, and Smith AL. 2011. gammadelta T cells play a protective role during infection with Nippostrongylus brasiliensis by promoting goblet cell function in the small intestine. Immunology 134: 448–458. [PubMed: 22044210]
21. Sharma A, Kumar P, and Ambasta RK. 2020. Cancer Fighting SiRNA-RRM2 Loaded Nanorobots. Pharm Nanotechnol 8: 79–90. [PubMed: 32003677]
22. Pflanz S, Timans JC, Cheung J, Rosales R, Kanzler H, Gilbert J, Hibbert L, Churakova T, Travis M, Vaisberg E, Blumenschein WM, Mattson JD, Wagner JL, To W, Zurawski S, McClanahan TK, Gorman DM, Bazan JF, de Waal Malefyt R, Rennick D, and Kastelein RA. 2002. IL-27, a heterodimeric cytokine composed of EBI3 and p28 protein, induces proliferation of naive CD4(+) T cells. Immunity 16: 779–790. [PubMed: 12121660]
23. Collison LW, Workman CJ, Kuo TT, Boyd K, Wang Y, Vignali KM, Cross R, Sehy D, Blumberg RS, and Vignali DA. 2007. The inhibitory cytokine IL-35 contributes to regulatory T-cell function. Nature 450: 566–569. [PubMed: 18033300]
24. Sharma A, Steven S, and Bosmann M. 2019. The pituitary gland prevents shock-associated death by controlling multiple inflammatory mediators. Biochem Biophys Res Commun 509: 188–193. [PubMed: 30579593]
25. Hamano S, Himeno K, Miyazaki Y, Ishii K, Yamanaka A, Takeda A, Zhang M, Hisaeda H, Mak TW, Yoshimura A, and Yoshida H. 2003. WSX-1 is required for resistance to Trypanosoma cruzi infection by regulation of proinflammatory cytokine production. Immunity 19: 657–667. [PubMed: 14614853]

26. Bosmann M, and Ward PA. 2013. Modulation of inflammation by interleukin-27. J Leukoc Biol 94: 1159–1165. [PubMed: 23904441]
27. Hunter CA, and Kastelein R. 2012. Interleukin-27: balancing protective and pathological immunity. Immunity 37: 960–969. [PubMed: 23244718]
28. Sharma A, Kontodimas K, and Bosmann M. 2021. The MAVS Immune Recognition Pathway in Viral Infection and Sepsis. Antioxid Redox Signal.
29. McHedlidze T, Kindermann M, Neves AT, Voehringer D, Neurath MF, and Wirtz S. 2016. IL-27 suppresses type 2 immune responses in vivo via direct effects on group 2 innate lymphoid cells. Mucosal Immunol 9: 1384–1394. [PubMed: 26982595]
30. Artis D, Villarino A, Silverman M, He W, Thornton EM, Mu S, Summer S, Covey TM, Huang E, Yoshida H, Koretzky G, Goldschmidt M, Wu GD, de Sauvage F, Miller HR, Saris CJ, Scott P, and Hunter CA. 2004. The IL-27 receptor (WSX-1) is an inhibitor of innate and adaptive elements of type 2 immunity. J Immunol 173: 5626–5634. [PubMed: 15494513]
31. Moro K, Kabata H, Tanabe M, Koga S, Takeno N, Mochizuki M, Fukunaga K, Asano K, Betsuyaku T, and Koyasu S. 2016. Interferon and IL-27 antagonize the function of group 2 innate lymphoid cells and type 2 innate immune responses. Nat Immunol 17: 76–86. [PubMed: 26595888]
32. Oshiro I, Takenaka T, and Maeda J. 1982. New method for hemoglobin determination by using sodium lauryl sulfate (SLS). Clin Biochem 15: 83–88. [PubMed: 7094292]
33. Bosmann M, Russkamp NF, Patel VR, Zetoune FS, Sarma JV, and Ward PA. 2011. The outcome of polymicrobial sepsis is independent of T and B cells. Shock 36: 396–401. [PubMed: 21701414]
34. Yoshida H, Hamano S, Senaldi G, Covey T, Faggioni R, Mu S, Xia M, Wakeham AC, Nishina H, Potter J, Saris CJ, and Mak TW. 2001. WSX-1 is required for the initiation of Th1 responses and resistance to L. major infection. Immunity 15: 569–578. [PubMed: 11672539]
35. Batten M, Li J, Yi S, Kljavin NM, Danilenko DM, Lucas S, Lee J, de Sauvage FJ, and Ghilardi N. 2006. Interleukin 27 limits autoimmune encephalomyelitis by suppressing the development of interleukin 17-producing T cells. Nature Immunology 7: 929–936. [PubMed: 16906167]
36. Stumhofer JS, Laurence A, Wilson EH, Huang E, Tato CM, Johnson LM, Villarino AV, Huang Q, Yoshimura A, Sehy D, Saris CJ, O'Shea JJ, Hennighausen L, Ernst M, and Hunter CA. 2006. Interleukin 27 negatively regulates the development of interleukin 17-producing T helper cells during chronic inflammation of the central nervous system. Nat Immunol 7: 937–945. [PubMed: 16906166]
37. Stumhofer JS, Silver JS, Laurence A, Porrett PM, Harris TH, Turka LA, Ernst M, Saris CJ, O'Shea JJ, and Hunter CA. 2007. Interleukins 27 and 6 induce STAT3-mediated T cell production of interleukin 10. Nat Immunol 8: 1363–1371. [PubMed: 17994025]
38. Kabelitz D, and Wesch D. 2003. Features and functions of gamma delta T lymphocytes: focus on chemokines and their receptors. Crit Rev Immunol 23: 339–370. [PubMed: 15030305]
39. Hughes CE, and Nibbs RJB. 2018. A guide to chemokines and their receptors. FEBS J 285: 2944–2971. [PubMed: 29637711]
40. Alflen A, Aranda Lopez P, Hartmann AK, Maxeiner J, Bosmann M, Sharma A, Platten J, Ries F, Beckert H, Ruf W, and Radsak MP. 2020. Neutrophil extracellular traps impair fungal clearance in a mouse model of invasive pulmonary aspergillosis. Immunobiology 225: 151867. [PubMed: 31761474]
41. Hazawa M, Lin DC, Handral H, Xu L, Chen Y, Jiang YY, Mayakonda A, Ding LW, Meng X, Sharma A, Samuel S, Movahednia MM, Wong RW, Yang H, Tong C, and Koeffler HP. 2017. ZNF750 is a lineage-specific tumour suppressor in squamous cell carcinoma. Oncogene 36: 2243–2254. [PubMed: 27819679]
42. Lin DC, Meng X, Hazawa M, Nagata Y, Varela AM, Xu L, Sato Y, Liu LZ, Ding LW, Sharma A, Goh BC, Lee SC, Petersson BF, Yu FG, Macary P, Oo MZ, Ha CS, Yang H, Ogawa S, Loh KS, and Koeffler HP. 2014. The genomic landscape of nasopharyngeal carcinoma. Nat Genet 46: 866–871. [PubMed: 24952746]
43. Hoyler T, Klose CS, Souabni A, Turqueti-Neves A, Pfeifer D, Rawlins EL, Voehringer D, Busslinger M, and Diefenbach A. 2012. The transcription factor GATA-3 controls cell fate and maintenance of type 2 innate lymphoid cells. Immunity 37: 634–648. [PubMed: 23063333]

44. Huang Y, Guo L, Qiu J, Chen X, Hu-Li J, Siebenlist U, Williamson PR, Urban JF Jr., and Paul WE. 2015. IL-25-responsive, lineage-negative KLRG1(hi) cells are multipotential 'inflammatory' type 2 innate lymphoid cells. Nat Immunol 16: 161–169. [PubMed: 25531830]
45. Kang Z, Swaidani S, Yin W, Wang C, Barlow JL, Gulen MF, Bulek K, Do JS, Aronica M, McKenzie AN, Min B, and Li X. 2012. Epithelial cell-specific Act1 adaptor mediates interleukin-25-dependent helminth expulsion through expansion of Lin(−)c-Kit(+) innate cell population. Immunity 36: 821–833. [PubMed: 22608496]
46. Price AE, Liang HE, Sullivan BM, Reinhardt RL, Eisley CJ, Erle DJ, and Locksley RM. 2010. Systemically dispersed innate IL-13-expressing cells in type 2 immunity. Proc Natl Acad Sci U S A 107: 11489–11494. [PubMed: 20534524]
47. Turner JE, Morrison PJ, Wilhelm C, Wilson M, Ahlfors H, Renauld JC, Panzer U, Helmby H, and Stockinger B. 2013. IL-9-mediated survival of type 2 innate lymphoid cells promotes damage control in helminth-induced lung inflammation. J Exp Med 210: 2951–2965. [PubMed: 24249111]
48. Van Dyken SJ, Nussbaum JC, Lee J, Molofsky AB, Liang HE, Pollack JL, Gate RE, Haliburton GE, Ye CJ, Marson A, Erle DJ, and Locksley RM. 2016. A tissue checkpoint regulates type 2 immunity. Nat Immunol 17: 1381–1387. [PubMed: 27749840]
49. Yang B, Suwanpradid J, Sanchez-Lagunes R, Choi HW, Hoang P, Wang D, Abraham SN, and MacLeod AS. 2017. IL-27 Facilitates Skin Wound Healing through Induction of Epidermal Proliferation and Host Defense. J Invest Dermatol 137: 1166–1175. [PubMed: 28132857]
50. Bouchery T, Coakley G, and Harris NL. 2020. Preparation of Nippostrongylus brasiliensis Larvae for the Study of Host Skin Response. Bio Protoc 10: e3849.
51. Obata-Ninomiya K, Ishiwata K, Tsutsui H, Nei Y, Yoshikawa S, Kawano Y, Minegishi Y, Ohta N, Watanabe N, Kanuka H, and Karasuyama H. 2013. The skin is an important bulwark of acquired immunity against intestinal helminths. J Exp Med 210: 2583–2595. [PubMed: 24166714]
52. Huang J, Hume AJ, Abo KM, Werder RB, Villacorta-Martin C, Alysandratos KD, Beermann ML, Simone-Roach C, Lindstrom-Vautrin J, Olejnik J, Suder EL, Bullitt E, Hinds A, Sharma A, Bosmann M, Wang R, Hawkins F, Burks EJ, Saeed M, Wilson AA, Muhlberger E, and Kotton DN. 2020. SARS-CoV-2 Infection of Pluripotent Stem Cell-Derived Human Lung Alveolar Type 2 Cells Elicits a Rapid Epithelial-Intrinsic Inflammatory Response. Cell Stem Cell 27: 962–973 e967. [PubMed: 32979316]
53. Schmidt-Wolf IG, Negrin RS, Kiem HP, Blume KG, and Weissman IL. 1991. Use of a SCID mouse/human lymphoma model to evaluate cytokine-induced killer cells with potent antitumor cell activity. J Exp Med 174: 139–149. [PubMed: 1711560]
54. Meresse B, Chen Z, Ciszewski C, Tretiakova M, Bhagat G, Krausz TN, Raulet DH, Lanier LL, Groh V, Spies T, Ebert EC, Green PH, and Jabri B. 2004. Coordinated induction by IL15 of a TCR-independent NKG2D signaling pathway converts CTL into lymphokine-activated killer cells in celiac disease. Immunity 21: 357–366. [PubMed: 15357947]
55. Avanzi GC, Cessano A, Brizzi MF, Clark SC, Pegoraro L, and Matera L. 1989. Biological and molecular evidence for the production of IL-6 by human natural killer cells in culture. Life Sci 45: 2621–2626. [PubMed: 2693867]
56. Kuhn KA, Manieri NA, Liu TC, and Stappenbeck TS. 2014. IL-6 stimulates intestinal epithelial proliferation and repair after injury. PLoS One 9: e114195. [PubMed: 25478789]
57. Saito F, Tasaka S, Inoue K, Miyamoto K, Nakano Y, Ogawa Y, Yamada W, Shiraishi Y, Hasegawa N, Fujishima S, Takano H, and Ishizaka A. 2008. Role of interleukin-6 in bleomycin-induced lung inflammatory changes in mice. Am J Respir Cell Mol Biol 38: 566–571. [PubMed: 18096870]
58. Bhargava R, Janssen W, Altmann C, Andres-Hernando A, Okamura K, Vandivier RW, Ahuja N, and Faubel S. 2013. Intratracheal IL-6 protects against lung inflammation in direct, but not indirect, causes of acute lung injury in mice. PLoS One 8: e61405. [PubMed: 23667439]
59. Sozzani S, Zhou D, Locati M, Rieppi M, Proost P, Magazin M, Vita N, van Damme J, and Mantovani A. 1994. Receptors and transduction pathways for monocyte chemotactic protein-2 and monocyte chemotactic protein-3. Similarities and differences with MCP-1. J Immunol 152: 3615–3622. [PubMed: 8144937]

60. Franci C, Wong LM, Van Damme J, Proost P, and Charo IF. 1995. Monocyte chemoattractant protein-3, but not monocyte chemoattractant protein-2, is a functional ligand of the human monocyte chemoattractant protein-1 receptor. J Immunol 154: 6511–6517. [PubMed: 7759884]

61. McKenzie DR, Kara EE, Bastow CR, Tyllis TS, Fenix KA, Gregor CE, Wilson JJ, Babb R, Paton JC, Kallies A, Nutt SL, Brustle A, Mack M, Comerford I, and McColl SR. 2017. IL-17-producing gammadelta T cells switch migratory patterns between resting and activated states. Nat Commun 8: 15632. [PubMed: 28580944]

62. McLoughlin RM, Jenkins BJ, Grail D, Williams AS, Fielding CA, Parker CR, Ernst M, Topley N, and Jones SA. 2005. IL-6 trans-signaling via STAT3 directs T cell infiltration in acute inflammation. Proc Natl Acad Sci U S A 102: 9589–9594. [PubMed: 15976028]

63. Barbi J, Oghumu S, Lezama-Davila CM, and Satoskar AR. 2007. IFN-gamma and STAT1 are required for efficient induction of CXC chemokine receptor 3 (CXCR3) on CD4+ but not CD8+ T cells. Blood 110: 2215–2216. [PubMed: 17785588]

64. Lanca T, Costa MF, Goncalves-Sousa N, Rei M, Grosso AR, Penido C, and Silva-Santos B. 2013. Protective role of the inflammatory CCR2/CCL2 chemokine pathway through recruitment of type 1 cytotoxic gammadelta T lymphocytes to tumor beds. J Immunol 190: 6673–6680. [PubMed: 23686489]

65. Penido C, Costa MF, Souza MC, Costa KA, Candea AL, Benjamim CF, and Henriques M. 2008. Involvement of CC chemokines in gammadelta T lymphocyte trafficking during allergic inflammation: the role of CCL2/CCR2 pathway. Int Immunol 20: 129–139. [PubMed: 18056919]

66. Xu P, Zhang F, Chang MM, Zhong C, Sun CH, Zhu HR, Yao JC, Li ZZ, Li ST, Zhang WC, and Sun GD. 2021. Recruitment of gammadelta T cells to the lesion via the CCL2/CCR2 signaling after spinal cord injury. J Neuroinflammation 18: 64. [PubMed: 33653377]

67. Bouchareychas L, Grossinger EM, Kang M, and Adamopoulos IE. 2018. gammadeltaTCR regulates production of interleukin-27 by neutrophils and attenuates inflammatory arthritis. Sci Rep 8: 7590. [PubMed: 29765156]

68. Morandi F, Prigione I, and Airoldi I. 2012. Human TCRgammadelta+ T cells represent a novel target for IL-27 activity. Eur J Immunol 42: 1547–1552. [PubMed: 22678908]

69. Iwasaki Y, Fujio K, Okamura T, and Yamamoto K. 2015. Interleukin-27 in T cell immunity. Int J Mol Sci 16: 2851–2863. [PubMed: 25633106]

70. Murugaiyan G, and Saha B. 2013. IL-27 in tumor immunity and immunotherapy. Trends Mol Med 19: 108–116. [PubMed: 23306374]

71. Mei Y, Lv Z, Xiong L, Zhang H, Yin N, and Qi H. 2021. The dual role of IL-27 in CD4+T cells. Mol Immunol 138: 172–180. [PubMed: 34438225]

72. Bosmann M, Russkamp NF, Strobl B, Roewe J, Balouzian L, Pache F, Radsak MP, van Rooijen N, Zetoune FS, Sarma JV, Nunez G, Muller M, Murray PJ, and Ward PA. 2014. Interruption of macrophage-derived IL-27(p28) production by IL-10 during sepsis requires STAT3 but not SOCS3. J Immunol 193: 5668–5677. [PubMed: 25348624]

73. Vijayan D, Mohd Redzwan N, Avery DT, Wirasinha RC, Brink R, Walters G, Adelstein S, Kobayashi M, Gray P, Elliott M, Wong M, King C, Vinuesa CG, Ghilardi N, Ma CS, Tangye SG, and Batten M. 2016. IL-27 Directly Enhances Germinal Center B Cell Activity and Potentiates Lupus in Sanroque Mice. J Immunol 197: 3008–3017. [PubMed: 27619997]

74. Li JP, Wu H, Xing W, Yang SG, Lu SH, Du WT, Yu JX, Chen F, Zhang L, and Han ZC. 2010. Interleukin-27 as a negative regulator of human neutrophil function. Scand J Immunol 72: 284–292. [PubMed: 20883313]

75. Ruckerl D, Hessmann M, Yoshimoto T, Ehlers S, and Holscher C. 2006. Alternatively activated macrophages express the IL-27 receptor alpha chain WSX-1. Immunobiology 211: 427–436. [PubMed: 16920482]

76. Perrigoue JG, Marshall FA, and Artis D. 2008. On the hunt for helminths: innate immune cells in the recognition and response to helminth parasites. Cell Microbiol 10: 1757–1764. [PubMed: 18505479]

77. McGuinness DH, Dehal PK, and Pleass RJ. 2003. Pattern recognition molecules and innate immunity to parasites. Trends Parasitol 19: 312–319. [PubMed: 12855382]

78. Leister H, Luu M, Staudenraus D, Lopez Krol A, Mollenkopf HJ, Sharma A, Schmerer N, Schulte LN, Bertrams W, Schmeck B, Bosmann M, Steinhoff U, and Visekruna A. 2021. Pro- and anti-tumorigenic capacity of immunoproteasomes in shaping the tumor microenvironment. Cancer Immunol Res.

79. Roewe J, Stavrides G, Strueve M, Sharma A, Marini F, Mann A, Smith SA, Kaya Z, Strobl B, Mueller M, Reinhardt C, Morrissey JH, and Bosmann M. 2020. Bacterial polyphosphates interfere with the innate host defense to infection. Nat Commun 11: 4035. [PubMed: 32788578]

80. Bosmann M, Haggadone MD, Hemmila MR, Zetoune FS, Sarma JV, and Ward PA. 2012. Complement activation product C5a is a selective suppressor of TLR4-induced, but not TLR3-induced, production of IL-27(p28) from macrophages. J Immunol 188: 5086–5093. [PubMed: 22491257]

81. Bosmann M, Strobl B, Kichler N, Rigler D, Grailer JJ, Pache F, Murray PJ, Muller M, and Ward PA. 2014. Tyrosine kinase 2 promotes sepsis-associated lethality by facilitating production of interleukin-27. J Leukoc Biol 96: 123–131. [PubMed: 24604832]

82. Lin DC, Xu L, Ding LW, Sharma A, Liu LZ, Yang H, Tan P, Vadgama J, Karlan BY, Lester J, Urban N, Schummer M, Doan N, Said JW, Sun H, Walsh M, Thomas CJ, Patel P, Yin D, Chan D, and Koeffler HP. 2013. Genomic and functional characterizations of phosphodiesterase subtype 4D in human cancers. Proc Natl Acad Sci U S A 110: 6109–6114. [PubMed: 23536305]

83. Schwacha MG, Rani M, Nicholson SE, Lewis AM, Holloway TL, Sordo S, and Cap AP. 2016. Dermal gammadelta T-Cells Can Be Activated by Mitochondrial Damage-Associated Molecular Patterns. PLoS One 11: e0158993. [PubMed: 27403524]

84. Villarino AV, Artis D, Bezbradica JS, Miller O, Saris CJ, Joyce S, and Hunter CA. 2008. IL-27R deficiency delays the onset of colitis and protects from helminth-induced pathology in a model of chronic IBD. Int Immunol 20: 739–752. [PubMed: 18375937]

85. Anuradha R, Munisankar S, Bhootra Y, Jagannathan J, Dolla C, Kumaran P, Shen K, Nutman TB, and Babu S. 2016. Systemic Cytokine Profiles in Strongyloides stercoralis Infection and Alterations following Treatment. Infect Immun 84: 425–431. [PubMed: 26597982]

86. Anuradha R, Munisankar S, Bhootra Y, Dolla C, Kumaran P, Nutman TB, and Babu S. 2017. Modulation of CD4(+) and CD8(+) T Cell Function and Cytokine Responses in Strongyloides stercoralis Infection by Interleukin-27 (IL-27) and IL-37. Infect Immun 85.

87. Hegewald J, Gantin RG, Lechner CJ, Huang X, Agosssou A, Agbeko YF, Soboslay PT, and Kohler C. 2015. Cellular cytokine and chemokine responses to parasite antigens and fungus and mite allergens in children co-infected with helminthes and protozoa parasites. J Inflamm (Lond) 12: 5. [PubMed: 25698903]

88. Pennock ND, Gapin L, and Kedl RM. 2014. IL-27 is required for shaping the magnitude, affinity distribution, and memory of T cells responding to subunit immunization. Proc Natl Acad Sci U S A 111: 16472–16477. [PubMed: 25267651]

89. Kilgore AM, Pennock ND, and Kedl RM. 2020. cDC1 IL-27p28 Production Predicts Vaccine-Elicited CD8(+) T Cell Memory and Protective Immunity. J Immunol 204: 510–517. [PubMed: 31871021]

90. Coffman RL, Sher A, and Seder RA. 2010. Vaccine adjuvants: putting innate immunity to work. Immunity 33: 492–503. [PubMed: 21029960]

91. Szabo PA, Miron M, and Farber DL. 2019. Location, location, location: Tissue resident memory T cells in mice and humans. Sci Immunol 4.

Key Points

- Deletion of IL-27RA confers susceptibility to primary hookworm lung infection.
- Recombinant IL-27 treatment reduces lung parasite burden and injury in mice.
- IL-27 promotes anti-helminthic responses via IL-27RA^{+} γδ T cells in the lungs.

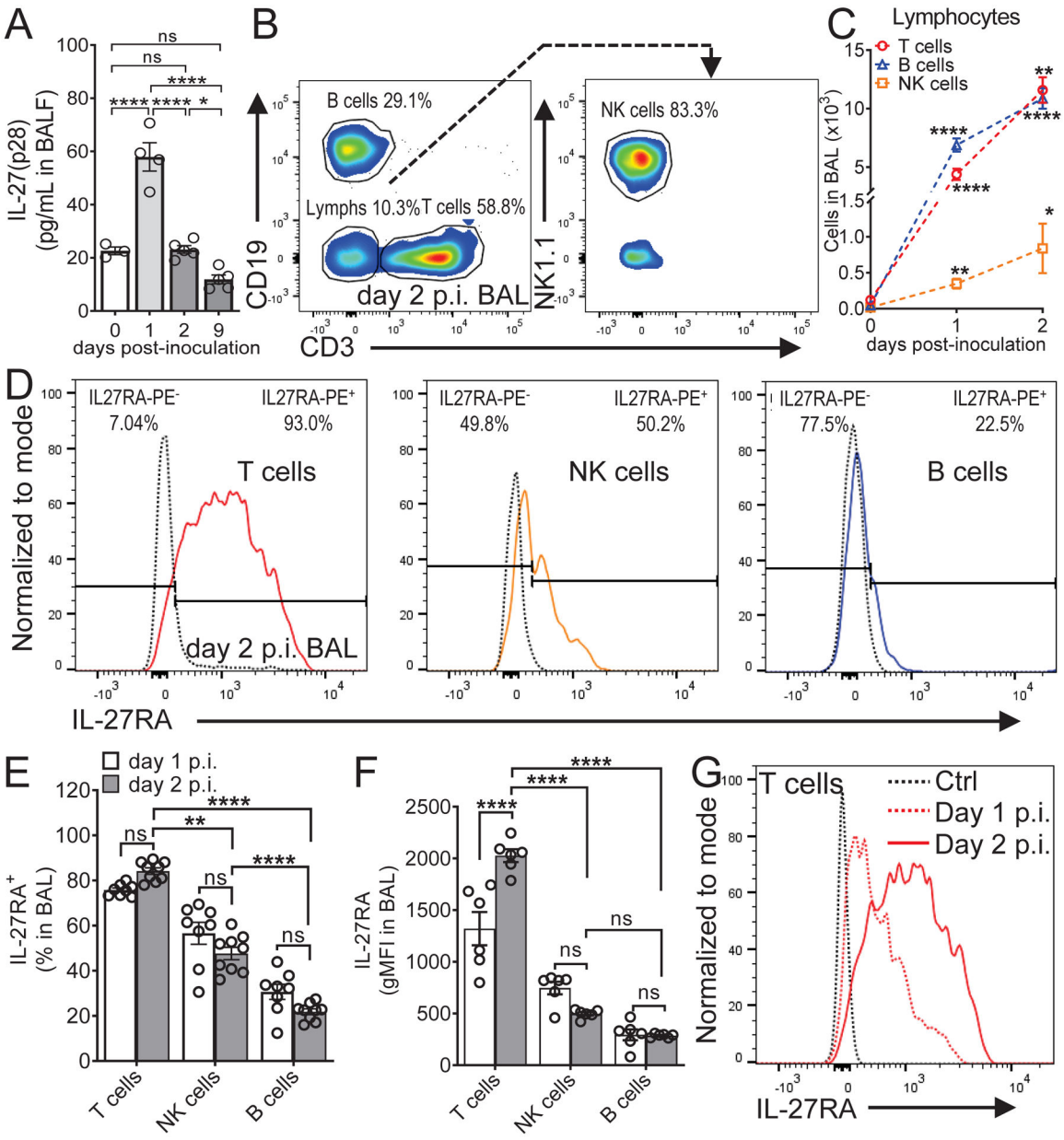

FIGURE 1.

N. brasiliensis infection promotes IL-27(p28) release and IL-27RA-expressing lymphocytes in the lungs.

C57BL/6J wild type (WT) mice were infected s.c. with third stage larvae (L3) of *N. brasiliensis* (n=500/mouse) or received a mock PBS injection as controls. The inflammatory cytokines or cells were collected by broncho-alveolar lavage (BAL). (**A**) IL-27(p28) was quantified in BAL fluid by ELISA at the indicated time points (n=3–5 mice/group). (**B**) Representative flow cytometry gating of CD19 versus CD3 pre-gated on $CD45^{+}Ly6G^{-}$ single cell lymphocytes (left panel), and NK1.1 versus CD3 gated on $CD19^{-}CD3^{-}$ innate lymphocytes (right panel), on day 2 post-inoculation (p.i.). Frequencies (%) of parent populations are indicated next to each gate. (**C**) Absolute numbers of lymphocyte

populations of $CD19^{-}CD3^{+}$ T cells, $CD19^{+}CD3^{-}$ B cells, and $CD19^{-}CD3^{-}NK1.1^{+}$ NK cells on days 0 (PBS-inoculated/uninfected), 1, and 2 p.i. (n=6–9 mice/group). (**D**) Representative histograms of IL-27RA expression on T cells (left panel), NK cells (middle panel), and B cells (right panel) on day 2 p.i. The dotted black line indicates isotype-FMO control. The frequencies of $IL\text{-}27RA^{-}$ and $IL\text{-}27RA^{+}$ cells are indicated in the upper left and right corners, respectively. (**E**) Frequencies of $IL\text{-}27RA^{+}$ T cells, NK cells, and B cells on days 1 and 2 p.i. (n=8–9 mice/group from 2 pooled experiments). (**F**) IL-27RA presence expressed as geometric mean fluorescence intensity (gMFI) on these cells at these time points (n=6 mice/group). (**G**) Representative histogram of IL-27RA expression on T cells on days 1 and 2 p.i. The dotted black line indicates isotype-FMO control (Ctrl). Each circle indicates an individual mouse (A, E, F). Data are shown as mean ± SEM (A, C, E, F). Data were analyzed by Student's t-test comparing day 0 vs. day 1 and day 0 vs. day 2 for each cell type (C), one-way ANOVA (A), or two-way ANOVA (E, F), * $P<0.05$, ** $P<0.01$, *** $P<0.001$, **** $P<0.0001$, ns: not significant.

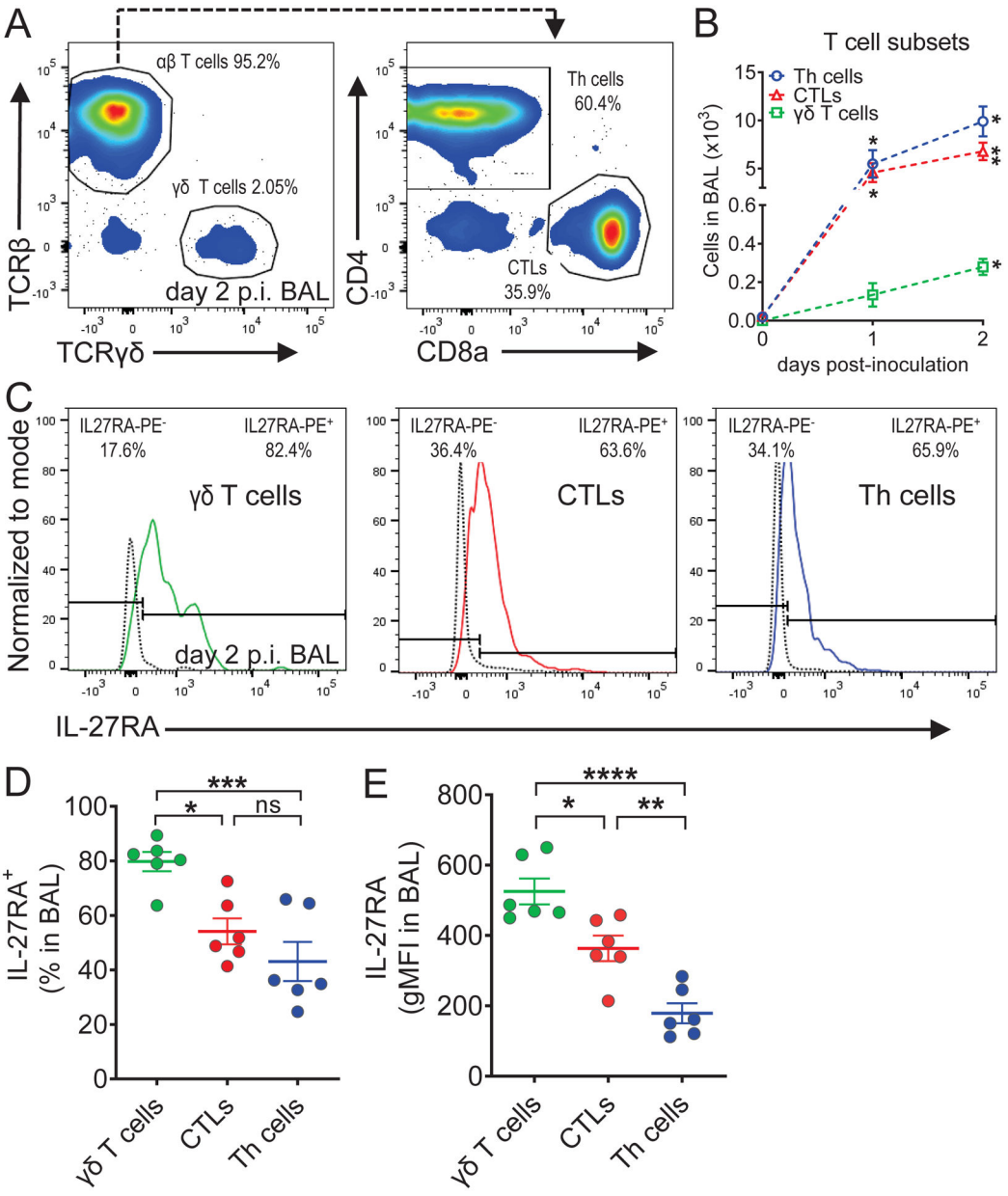

FIGURE 2.

IL-27RA expression is highest on γδ T cells among broncho-alveolar lymphocytes during *N. brasiliensis* infection.

C57BL/6J (WT) mice were infected s.c. with third stage larvae (L3) of *N. brasiliensis* (n=500/mouse) or received a mock PBS injection as controls. Cells were collected by BAL. (**A**) Representative flow cytometry gating of TCRβ chain versus TCRγδ chain pre-gated on $CD3^+$ single cell lymphocytes (left panel), and CD4 versus CD8a on αβ T cells (right panel), on day 2 p.i. Frequencies (%) of parent populations are indicated next to each gate. (**B**) Absolute numbers of $CD4^+CD8^-$ T helper (Th) cells, $CD4^-CD8^+$ cytotoxic T lymphocytes (CTLs), and $TCR\beta^-TCR\gamma\delta^+$ γδ T cells on day 0 (PBS-inoculated/uninfected), day 1 (n=2 mice/group), and day 2 (n=6 mice/group) p.i. (**C**) Representative histograms of

IL-27RA expression on γδ T cells (left panel), CTLs (middle panel), and Th cells (right panel). The dotted black line indicates IL-27RA staining in Il27ra$^{-/-}$ mice as a negative control. The frequencies of IL-27RA^{-} and IL-27RA^{+} cells are indicated in the upper left and right corners, respectively. (**D**) Frequencies of IL-27RA^{+} γδ T cells, CTLs, and Th cells on day 2 p.i. (n=6 mice/group). (**E**) IL-27RA abundance (gMFI) on γδ T cells, CTLs, and Th cells on day 2 p.i. (n=6 mice/group). Each circle indicates an individual mouse (D, E). Data are shown as mean ± SEM (B, D, E). Data were analyzed by Student's t-test comparing day 0 vs. day 1 and day 0 vs. day 2 for each cell type (B), or one-way ANOVA (D, E), * $P<0.05$, ** $P<0.01$, *** $P<0.001$, **** $P<0.0001$, ns: not significant.

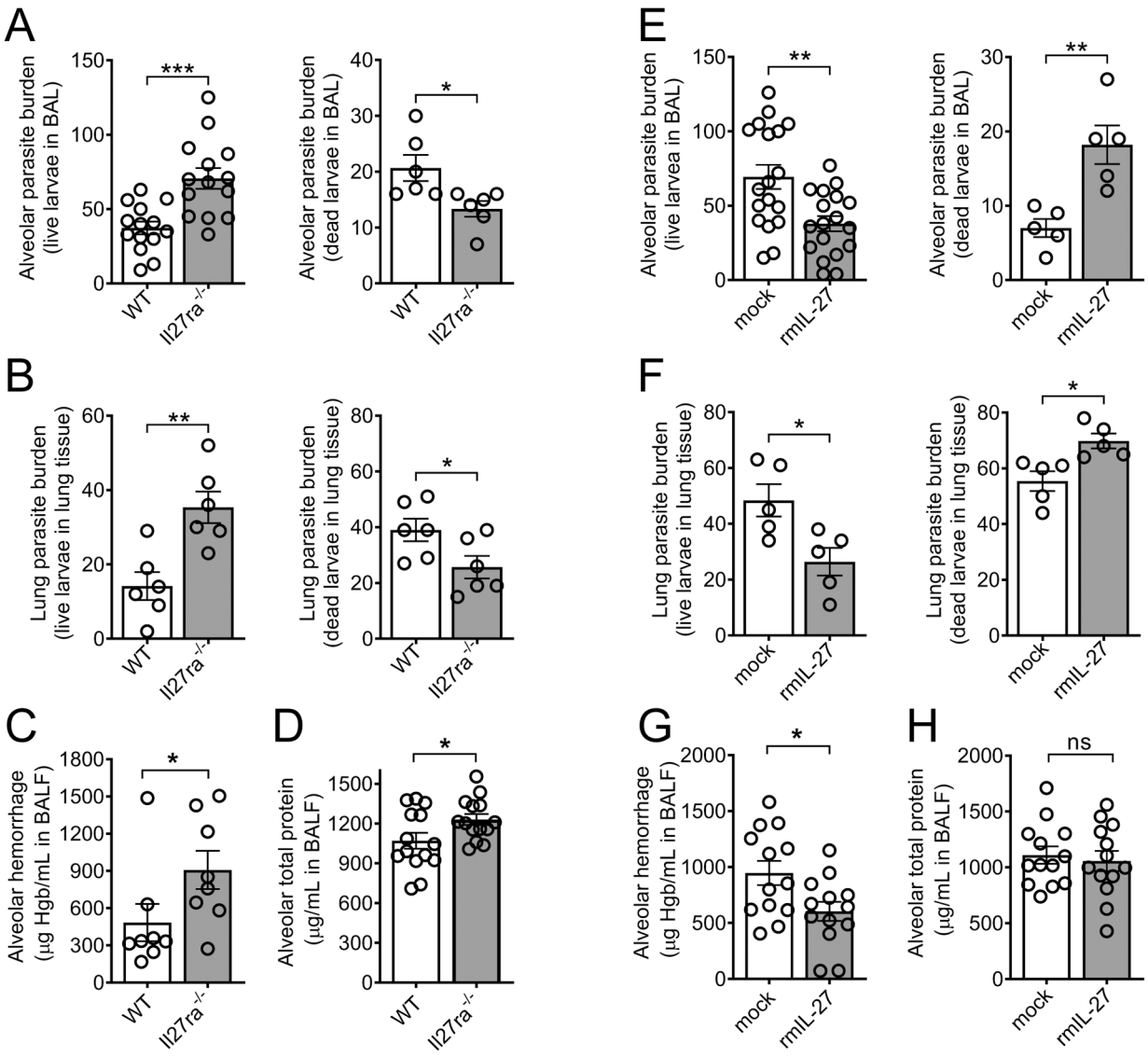

FIGURE 3.

IL-27 enhances innate resistance to primary *N. brasiliensis* infection in the lungs. (**A-D**) *In vivo* comparison of the susceptibility of Il27ra$^{-/-}$ mice and WT control (C57BL/6NJ) mice to primary *N. brasiliensis* infection (n=500 L3/mouse, s.c.) in the lungs on day 2 p.i. (**A**) Alveolar live and dead parasite burden in BAL (n=6–14 mice/group) and (**B**) parasite burden within lung tissue consisting of live and dead larvae (n=6 mice/group). (**C**) Alveolar hemorrhage (n=8 mice/group, and (**D**) alveolar total protein in BALF (n=14 mice/group). (**E-H**) *In vivo* comparison of the susceptibility of C57BL/6J mice administered rmIL-27 (100 ng/mouse) i.p. on days 0 and 1 p.i.) or mock control (0.1% BSA in PBS i.p.) to primary *N. brasiliensis* infection in the lungs on day 2 p.i. (**E**) Alveolar parasite burden in BAL and (**F**) lung parasite burden within tissue consisting of live and dead larvae (n=18 or n=5 mice/group). (**G**) Alveolar hemorrhage and (**H**) alveolar total protein in BALF (n=13 mice/group from 2 pooled experiments). Each circle indicates an individual mouse. Frames A, D, G-H are pooled from two independent experiments and data are shown as mean ±

SEM and were analyzed by Student's t-test, * $P<0.05$, ** $P<0.01$, *** $P<0.001$, ns: not significant.

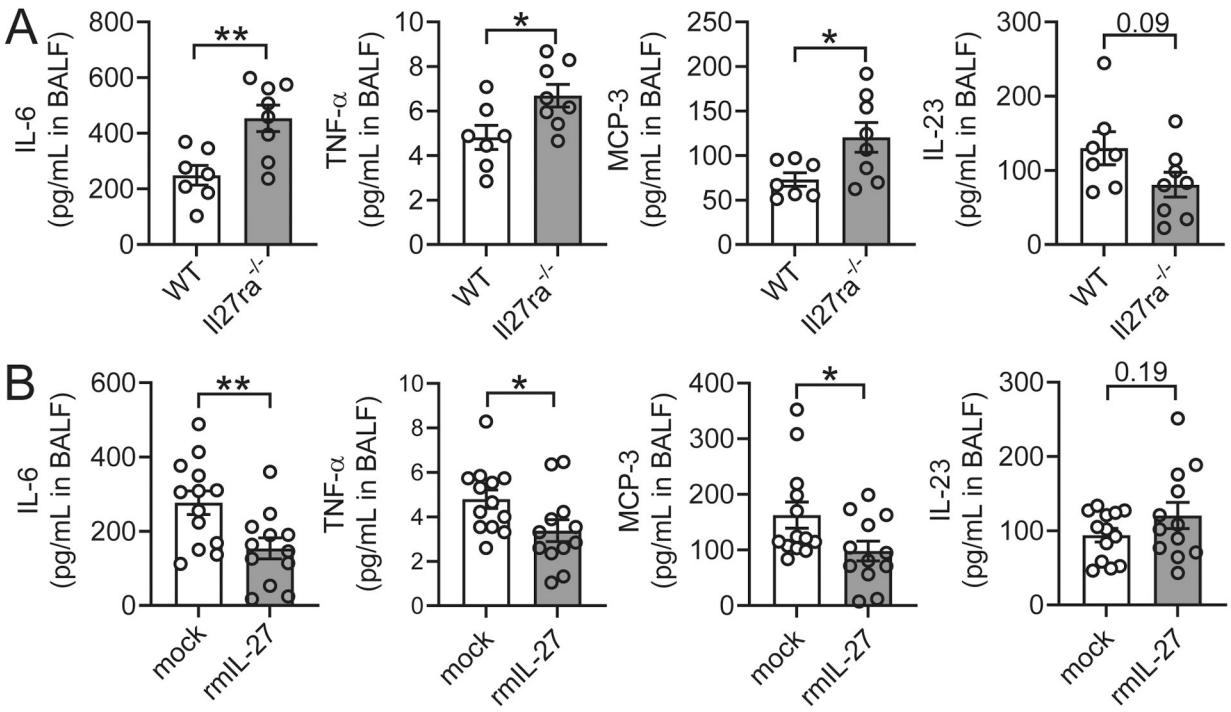

FIGURE 4.

IL-27 regulates inflammatory mediators during primary *N. brasiliensis* infection of the lungs.

(**A**) *In vivo* comparison of selected BALF cytokines and chemokines from Il27ra$^{-/-}$ mice and WT control (C57BL/6NJ) mice during primary *N. brasiliensis* infection (n=500 L3/mouse, s.c.) on day 2 p.i. (n=7–8 mice/group). (**B**) *In vivo* comparison of selected BALF cytokines and chemokines in WT (C57BL/6J) mice administered rmIL-27 (100 ng/mouse i.p on days 0 and 1 p.i.) or mock control (0.1% BSA in PBS i.p.) during primary *N. brasiliensis* infection on day 2 p.i. (n=12–13 mice/group from 2 pooled experiments). All data were obtained by bead-based multiplex assay (Luminex-200). Each circle indicates an individual mouse. Data are shown as mean ± SEM and were analyzed by Student's t-test, * $P<0.05$, ** $P<0.01$.

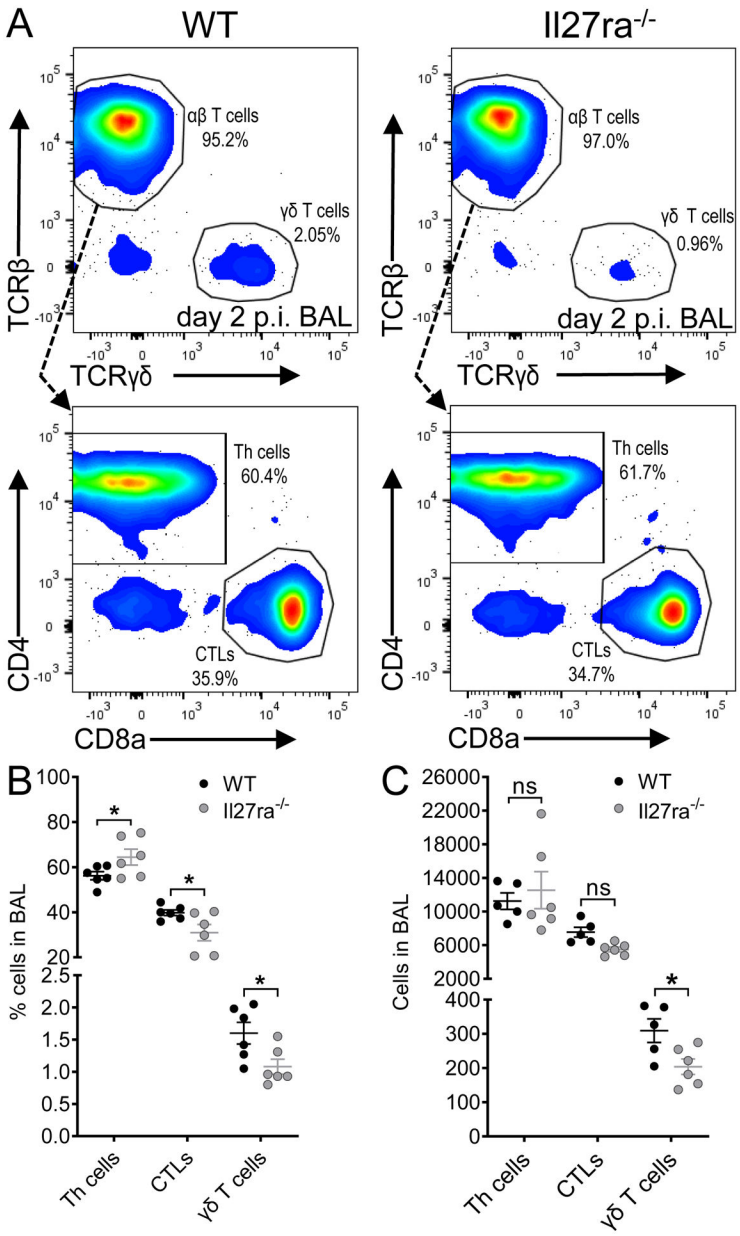

FIGURE 5.

Il27ra$^{-/-}$ mice have decreased presence of γδ T cells in the alveolar space during *N. brasiliensis* infection.

(**A**) Representative flow cytometry gating of TCRβ^{-}TCRγδ^{+} γδ T cells (top panels), CD4^{+}CD8^{-} Th cells, and CD4^{-}CD8^{+} CTLs (bottom panels), from WT control (C57BL/6NJ) (left panels) and Il27ra$^{-/-}$ mice (right panels) in BAL during *N. brasiliensis* infection (n=500 L3/mouse, s.c.) on day 2 p.i. Frequencies (%) of parent populations are indicated next to each gate. Cells were pre-gated on live singlet lymphocytes. (**B**) Frequencies and (**C**) absolute numbers of these CD4^{+}CD8^{-} Th cells, CD4^{-}CD8^{+} CTLs, and TCRβ^{-}TCRγδ^{+} γδ T cells in BAL of WT (n=5 mice/group; one mouse was removed due to extremely low infection, as determined by negligible hemorrhage) and Il27ra$^{-/-}$ (n=6 mice/group) mice on

day 2 p.i. Each circle indicates an individual mouse (B, C). Data are shown as mean ± SEM (B, C) and were analyzed by Student's t-test (B,C), * P<0.05, ns: not significant.

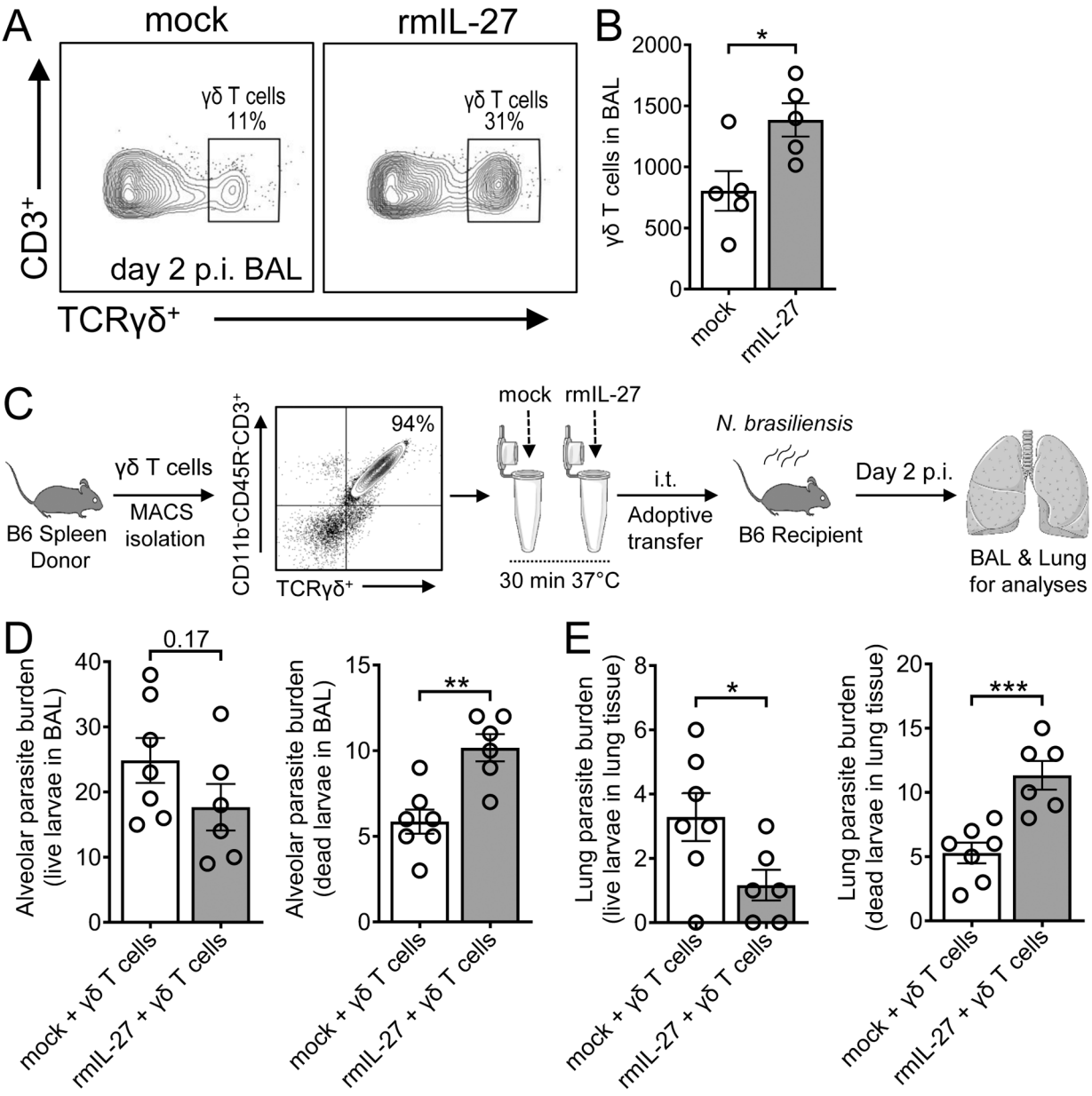

FIGURE 6.

IL-27 enhances γδ T cell-mediated innate resistance to primary *N. brasiliensis* infection in the lungs.

(**A**-**B**) C57BL/6J (WT) mice were administered rmIL-27 (100 ng/mouse i.p. on days 0 and 1 p.i.) or mock control (0.1% BSA in PBS i.p.) during *N. brasiliensis* infection (n=500 L3/mouse, s.c.). γδ T cells were analyzed on day 2 p.i in BAL. (**A**) Representative flow cytometry plots showing frequencies and (**B**) absolute numbers of $CD3^+$ $TCR\gamma\delta^+$ γδ T cells in the alveolar spaces of rm-IL27-treated mice (n=5 mice/group). (**C**) Workflow demonstrating γδ T cell adoptive transfer approach. γδ T cells ($CD11b^-CD45R^-CD3^+TCR\gamma\delta^+$) were positively selected from the spleens of naïve WT mice using magnetic beads (purity of $TCR\gamma\delta^+$ fraction ~95%), treated for 30 min at

37°C *in vitro* with mock (PBS) or rmIL-27 (100 ng/ml), washed thoroughly, and injected intratracheally into recipient mice 12 hours after inoculation with *N. brasiliensis*. (**D**) Alveolar parasite burden by BAL and (**E**) lung parasite burden within lung tissue consisting of live and dead larvae on day 2 p.i. following the adoptive transfer (n=6–7 mice/group). Each circle indicates an individual mouse (B, D, E). Data are shown as mean ± SEM (B, D, E) and were analyzed by Student's t-test, * P<0.05, ** P<0.01, *** P<0.001.